

Intestinal Insulin Resistance and Aberrant Production of Apolipoprotein B48 Lipoproteins in an Animal Model of Insulin Resistance and Metabolic Dyslipidemia

Evidence for Activation of Protein Tyrosine Phosphatase-1B, Extracellular Signal-Related Kinase, and Sterol Regulatory Element-Binding Protein-1c in the Fructose-Fed Hamster Intestine

Lisa M. Federico, Mark Naples, Denise Taylor, and Khosrow Adeli

Postprandial dyslipidemia is recognized as an important complication of insulin-resistant states, and recent evidence implicates intestinal lipoprotein overproduction as a causative factor. The mechanisms linking intestinal lipoprotein overproduction and aberrant insulin signaling in intestinal enterocytes are currently unknown. Intestinal insulin sensitivity and lipid metabolism were studied in a fructose-fed hamster model of insulin resistance and metabolic dyslipidemia. Intestinal lipoprotein production in chow-fed hamsters was responsive to the inhibitory effects of insulin, and a decrease in circulating levels of triglyceride-rich apolipoprotein (apo)B48-containing lipoproteins occurred 60 min after insulin administration. However, fructose-fed hamster intestine was not responsive to the insulin-induced downregulation of apoB48-lipoprotein production, suggesting insulin insensitivity at the level of the intestine. Enterocytes from the fructose-fed hamster exhibited normal activity of the insulin receptor but reduced levels of insulin receptor substrate-1 phosphorylation and mass and Akt protein mass. Conversely, the protein mass of the p110 subunit of phosphatidylinositol 3-kinase, protein tyrosine phosphatase-1B, and basal levels of phosphorylated extracellular signal-related kinase (ERK) were significantly increased in the fructose-fed hamster intestine. Modulating the ERK pathway through *in vivo* inhibition of mitogen-activated protein/ERK kinase 1/2, the upstream activator of ERK1/2, we observed a significant decrease in intestinal apoB48 synthesis and secretion. Interestingly,

enhanced basal ERK activity in the fructose-fed hamster intestine was accompanied by an increased activation of sterol regulatory element-binding protein. In summary, these data suggest that insulin insensitivity at the level of the intestine and aberrant insulin signaling are important underlying factors in intestinal overproduction of highly atherogenic apoB48-containing lipoproteins in the insulin-resistant state. Basal activation of the ERK pathway may be an important contributor to the aberrant insulin signaling and lipoprotein overproduction in this model. *Diabetes* 55:1316–1326, 2006

The insulin-resistant state is associated with a cluster of pathologies often referred to as the metabolic syndrome (1). The various pathologies include obesity, hypertension, dyslipidemia, and atherosclerosis (2,3). There is heightened awareness regarding the diagnosis and assessment of insulin-resistant states because insulin resistance is now recognized to be a major causative factor in the development of human atherosclerosis and cardiovascular disease (CVD) (4). CVD has been identified as the principal clinical outcome of the metabolic syndrome (1) and the primary cause of death among diabetic patients (5).

A contributing factor to the development of CVD is the metabolic dyslipidemia associated with insulin resistance. Increasingly, postprandial lipemia is being recognized as an inherent feature of diabetic dyslipidemia and is highly prevalent in diabetic patients even with normal fasting triglyceride concentrations (6,7). The accumulation of remnant lipoproteins has been attributed to a decrease in their clearance as well as increased intestinal synthesis (8). To date, the majority of investigations have focused on the retarded plasma clearance of alimentary lipoproteins as an underlying mechanism for postprandial hypertriglyceridemia. There is now growing evidence that intestinal lipoprotein secretion may be a major contributor to the fasting and postprandial lipemia observed in insulin-resistant states (8–12). The assembly of chylomicrons requires

From the Clinical Biochemistry Division, Department of Laboratory Medicine and Pathobiology, Hospital for Sick Children, University of Toronto, Toronto, Ontario

Address correspondence and reprint requests to Khosrow Adeli, Division of Clinical Biochemistry DPLM, Hospital for Sick Children, 555 University Ave., Toronto, Ontario, Canada M5G 1X8. E-mail: k.adeli@utoronto.ca.

Received for publication 4 September 2004 and accepted in revised form 6 February 2006.

apo, apolipoprotein; CVD, cardiovascular disease; ERK, extracellular signal-related kinase; IRS, insulin receptor substrate; MAP, mitogen-activated protein; MEK, mitogen-activated protein/ERK kinase; PI, phosphatidylinositol; PTP, protein tyrosine phosphatase; SREBP, sterol regulatory element-binding protein; TNF, tumor necrosis factor.

DOI: 10.2337/db04-1084

© 2006 by the American Diabetes Association.

The costs of publication of this article were defrayed in part by the payment of page charges. This article must therefore be hereby marked "advertisement" in accordance with 18 U.S.C. Section 1734 solely to indicate this fact.

apolipoprotein (apo) B48. Synthesized exclusively in the intestine, apoB48 plays a critical role in the intestinal absorption of dietary triglycerides and cholesterol and has been shown to be a very useful indicator of intestinally derived lipoprotein particles (13). It has been widely established that insulin induces an inhibitory effect on the synthesis of hepatically derived apoB100 (14); however, there have been few studies regarding insulin's effect on intestinal apoB48. In diabetic and insulin-resistant states, an increase in apoB48 production has been observed. *Psammomys obesus*, a nutritionally induced model of insulin resistance and type 2 diabetes, experiences elevated apoB48 biogenesis and triglyceride-rich lipoprotein production (15). Furthermore, in non-insulin-dependent diabetic patients, increased fasting and postprandial triglyceride-rich lipoproteins were associated with increased apoB48 production (7,16).

The principal cellular mechanisms leading to insulin resistance are currently unknown but are believed to be the result of defects in the insulin signaling transduction cascade. Our laboratory has developed and extensively characterized a diet-induced animal model of insulin resistance, the fructose-fed Syrian golden hamster (17,18). Fructose feeding for a 2-week period induced whole-body insulin resistance accompanied by a considerable rise in the *in vivo* production of hepatic VLDL-apoB and -triglyceride. Using the fructose-fed animal model of insulin resistance, we also examined the cellular mechanisms of insulin resistance and characteristics of dyslipidemia in the liver. In the fructose-fed hamster, decreased activity of the insulin receptor, insulin receptor substrates (IRSs), and Akt as well as a significant overexpression of protein tyrosine phosphatase (PTP)-1B was observed in hepatocytes (19). Interestingly, the fructose-fed hamster model exhibited not only an overproduction of hepatically derived VLDL but also clear evidence of intestinal apoB48-lipoprotein overproduction (9,13). This overproduction of apoB48 was accompanied by enhanced intestinal *de novo* lipogenesis, elevated endogenous synthesis of triglyceride and cholesterol ester, and an increase in microsomal triglyceride transfer protein mass and activity (9). Collectively, these results suggest intestinal overproduction of apoB48-containing lipoproteins in the fructose-fed hamster model; however, little is known about the link between intestinal lipoprotein production and the insulin sensitivity observed in this model. Although there have been numerous studies of the insulin signaling cascade in the insulin-resistant state in known insulin-sensitive tissues such as the liver, muscle, and adipose (20–24), little is known regarding intestinal insulin signaling and potential perturbations in insulin resistance.

In the current study, we examined the effect of insulin on postprandial apoB48 accumulation in chow-fed and fructose-fed hamsters both *in vivo* and *ex vivo* in freshly isolated intestinal enterocytes. To assess intestinal insulin sensitivity, we measured the expression and activity of various components of the insulin signaling cascade in primary enterocytes. *In vivo* modulation of the intestinal insulin signaling cascade in the hamster model suggested a possible link between extracellular signal-related kinase (ERK) activation and apoB48 lipoprotein production.

RESEARCH DESIGN AND METHODS

Male Syrian golden hamsters from 80 to 100 g (*Mesocricetus auratus*; Charles River, Montreal, Quebec, Canada) were paired based on weight and age and placed on either chow diet or fructose-enriched diet (Dyets, Bethlehem, PA).

The diet was continued for 14 days *ad libitum*. The animals were fasted for 16 h before enterocyte isolation. The fructose-feeding protocol used in the current study was exactly the same as previously published protocols (18,19) and shown to cause an insulin-resistant state. To confirm whether insulin resistance had developed in these animals, we typically measured plasma insulin concentrations and found a significant elevation with fructose feeding (92.0 ± 15 pmol/l at baseline, 204.0 ± 28 pmol/l after 2 weeks of fructose feeding, $P < 0.05$, $n = 4$). No significant difference in body weight was observed after fructose feeding (135.6 ± 11.1 vs. 133.2 ± 13.3 g). As expected, fructose feeding increased plasma lipids (cholesterol: from 2.89 ± 0.43 to 3.60 ± 0.35 mmol/l, $n = 10$, $P < 0.001$; triglycerides: from 1.16 ± 0.31 to 2.07 ± 0.85 mmol/l, $n = 6$, $P < 0.05$).

In vivo insulin treatment. Hamsters were anesthetized and given a fat load (200 μ l olive oil) via oral gavage. After 20 min, animals were injected with Triton WR-1339 and either saline (0.9% NaCl) or insulin (5 units/kg) into the jugular vein, and 400 μ l of blood was collected as a baseline reading. Blood collections (400 μ l) continued every 30 min for 90 min. Then, 50 μ l of 0.5 mol/l EDTA was added to inhibit clotting. Intestine was excised after the 90-min period for metabolic labeling experiments.

Enterocyte insulin treatment. Enterocytes were isolated from chow-fed and fructose-fed hamsters as previously described (9). Enterocytes were incubated in insulin-free Dulbecco's modified Eagle's medium for 1–3 h. Cells were stimulated with 100 nmol/l insulin for 2–10 min, washed twice with ice-cold PBS, and lysed using phosphate-free cell solubilizing buffer (150 mmol/l NaCl, 10 mmol/l Tris, pH 7.4, 1 mmol/l EDTA, 1 mmol/l EGTA, 2 mmol/l phenylmethylsulfonyl fluoride, 10 μ g/ml aprotinin, 100 mmol/l sodium fluoride, 10 mmol/l sodium pyrophosphate, and 2 mmol/l sodium orthovanadate).

In vivo mitogen-activated protein/ERK kinase 1/2 inhibition. Chow-fed hamsters (80–100 g) were injected intraperitoneally with 13.5 mg/kg PD98059 (dissolved in DMSO) and fasted overnight. Two hours before being killed, hamsters were injected intraperitoneally with 6.5 mg/kg PD98059 (Calbiochem, San Diego, CA). Control hamsters were injected with equal volumes of DMSO. The intestine was excised and washed, and the enterocytes were isolated for metabolic labeling and insulin stimulation.

Isolating triglyceride-rich lipoproteins. To isolate the triglyceride-rich lipoprotein fraction, blood was centrifuged at 4°C for 15 min at 5,000 rpm, and the plasma layer was separated. Then, 200 μ l of plasma was centrifuged at 100,000g for 70 min at 15°C in a 5-ml ultracentrifuge tube overlaid with 4 ml KBr solution (density 1.0006 g/ml). We removed the top layer (400 μ l) containing the triglyceride-rich lipoproteins (Svedberg flotation unit [S_0] 20–40). Then, 140 μ l of the triglyceride-rich lipoprotein fraction was added to 50 μ l sample buffer. The samples were vortexed and boiled for 5 min at 100°C. Finally, 10–20 μ l of sample was used for SDS-PAGE.

PTP-1B activity assay. Primary enterocytes isolated from chow-fed and fructose-fed hamsters were lysed and equal amounts of total protein subjected to immunoprecipitation using a monoclonal PTP-1B antibody (Oncogene). After immunoprecipitation and washing, the beads were incubated for 1 h at 30°C in PTP-1B assay buffer containing 200 μ mol/l epidermal growth factor receptor (a substrate for PTP-1B). After this step, samples were centrifuged (13,000 rpm, 3 min), and PTP-1B activity was assessed by quantifying the amount of free phosphate present in supernatants. This was done using a commercially available reagent and phosphate standards as per the manufacturer's instructions (Biomol Green Reagent; Biomol). All activity assays were performed in quadruplicate ($n = 5$).

Metabolic labeling of intact primary enterocytes. Primary hamster enterocytes were pulse labeled as previously described (9) with minor alterations. Briefly, cells were preincubated in methionine-free Dulbecco's modified Eagle's medium at 37°C for 45 min and pulsed with 30 μ Ci/ml of [35 S]methionine for 60 min. The cells and media were harvested and lysed, and apoB48 was immunoprecipitated.

Preparation of microsomes. Enterocytes were homogenized, using a Potter Elvehjem homogenizer in a homogenization medium of 0.25 mol/l sucrose and 10 mmol/l Tris-HCl, pH 7.4. Lysate was centrifuged at 12,000g for 20 min. The supernatant was then centrifuged at 100,000g for 45 min. The pellet was solubilized in cell solubilizing buffer before immunoblot analysis for mature and immature forms of sterol regulatory element-binding protein (SREBP)-1c.

Immunoprecipitation, SDS-PAGE, and immunoblotting. Immunoprecipitation, SDS-PAGE, and immunoblotting were performed essentially as previously described (9).

Statistical analysis. Statistical significance was calculated, using a two-tailed paired Student's *t* test analysis or one-way ANOVA. *P* values <0.05 were considered significant.

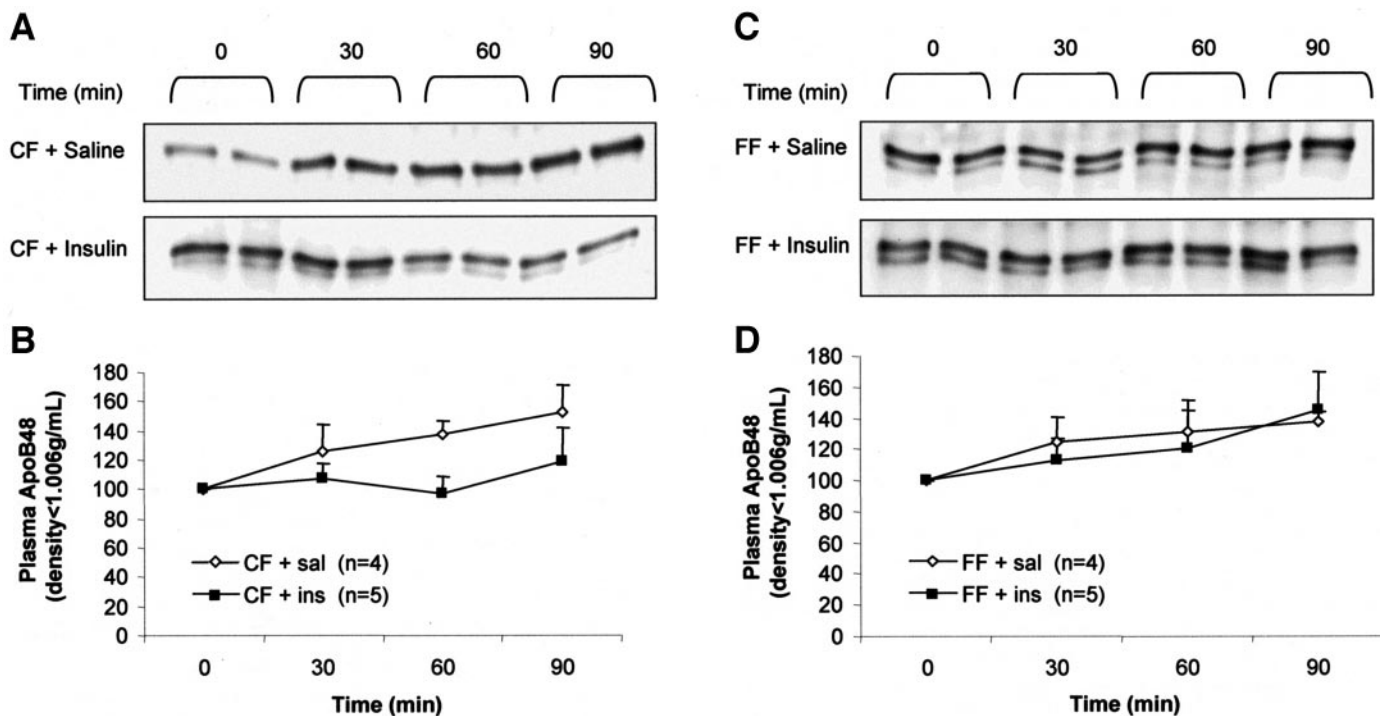


FIG. 1. Insulin treatment decreases circulating apoB48-containing lipoproteins in the chow-fed (CF) hamster but does not affect circulating apoB48-containing lipoproteins in the fructose-fed (FF) hamster. Triglyceride-rich lipoproteins were collected at 0, 30, 60, and 90 min from saline-treated and insulin-treated hamsters. Triglyceride-rich lipoproteins were immunoblotted, using an anti-hamster apoB antibody. Shown are representative immunoblots for chow-fed (A) and fructose-fed (C) hamsters. B and D: Graphical representation of apoB48 in the triglyceride-rich lipoprotein fraction. Immunoblots were analyzed using densitometry and expressed as a percentage of time 0 (means \pm SD). * $P < 0.05$. ins, insulin; sal, saline.

RESULTS

Acute insulin treatment inhibits postprandial accumulation of apoB48-containing lipoproteins in the chow-fed hamster; however, the fructose-fed hamster is resistant to the inhibitory effects of insulin. To investigate the effect of insulin on circulating apoB48-containing lipoproteins, chow-fed hamsters were given an oral fat load followed by an intravenous insulin injection. Hamsters were also given an intravenous Triton WR-1339 injection to inhibit the formation of chylomicron remnants and to inhibit uptake into the liver via the inhibition of lipoprotein lipase (15,25). Plasma was collected at times 0, 30, 60, and 90 min after insulin treatment, and the triglyceride-rich lipoprotein fraction (density < 1.006 g/ml) was isolated by ultracentrifugation. An analysis of circulating apoB48-containing lipoproteins indicated that insulin was able to inhibit the accumulation of chylomicrons in the bloodstream. In the saline-treated hamsters, the amount of apoB48-containing lipoproteins continued to increase throughout the 90-min time period. This increasing trend was not evident in the insulin-treated group compared with the control group. Comparing the rate of apoB48 accumulation in the plasma over the 90-min time period, there was a significantly decreased accumulation of apoB48-containing lipoproteins ($P = 0.02$) in insulin-treated hamsters. At time 60 min, there was a significant decrease in plasma apoB48-containing lipoproteins in the insulin-treated hamster (40% decrease, $P < 0.05$) (Fig. 1A and B).

We also investigated whether insulin can decrease circulating apoB48-containing lipoproteins in the insulin-resistant fructose-fed hamster model. Identical experiments were performed, using the insulin-resistant fructose-fed ham-

ster model. Throughout the 90-min time period, in both saline-treated and insulin-treated fructose-fed hamsters, apoB48-containing lipoproteins continued to increase in the circulation. There was no significant difference in the accumulation of apoB48-containing lipoprotein between the two groups (Fig. 1C and D).

Acute insulin treatment decreases apoB48 secretion from enterocytes in the chow-fed hamster, whereas enterocytes from the fructose-fed hamster are resistant to the inhibitory effects of insulin. To investigate whether insulin decreases the production of apoB48-containing lipoproteins at the level of the enterocyte, we examined the synthesis and secretion of apoB48 *ex vivo* in enterocytes isolated from saline-treated and insulin-treated chow-fed and fructose-fed animals. Enterocytes were isolated from saline-treated and insulin-treated hamsters and radiolabeled with [35 S]methionine for 60 min. In the insulin-treated chow-fed hamsters, a decreasing trend was observed in the levels of cellular apoB, which approached significance ($P = 0.07$). However, insulin significantly inhibited the amount of apoB48 secreted into the media ($56.2 \pm 1.2\%$, $P = 0.01$) (Fig. 2A and B). In the fructose-fed hamster model, insulin treatment did not affect apoB48 synthesis or secretion in intestinal enterocytes (Fig. 2C and D).

Ex vivo insulin stimulation and tyrosine phosphorylation of the insulin receptor in chow-fed and fructose-fed hamster enterocytes. To assess whether hamster intestinal enterocytes are responsive to insulin, we treated enterocytes with 100 nmol/l insulin for 10 min, immunoprecipitated the insulin receptor, and immunoblotted for phosphorylated tyrosine and insulin receptor mass. After a 10-min 100 nmol/l insulin treatment, we were

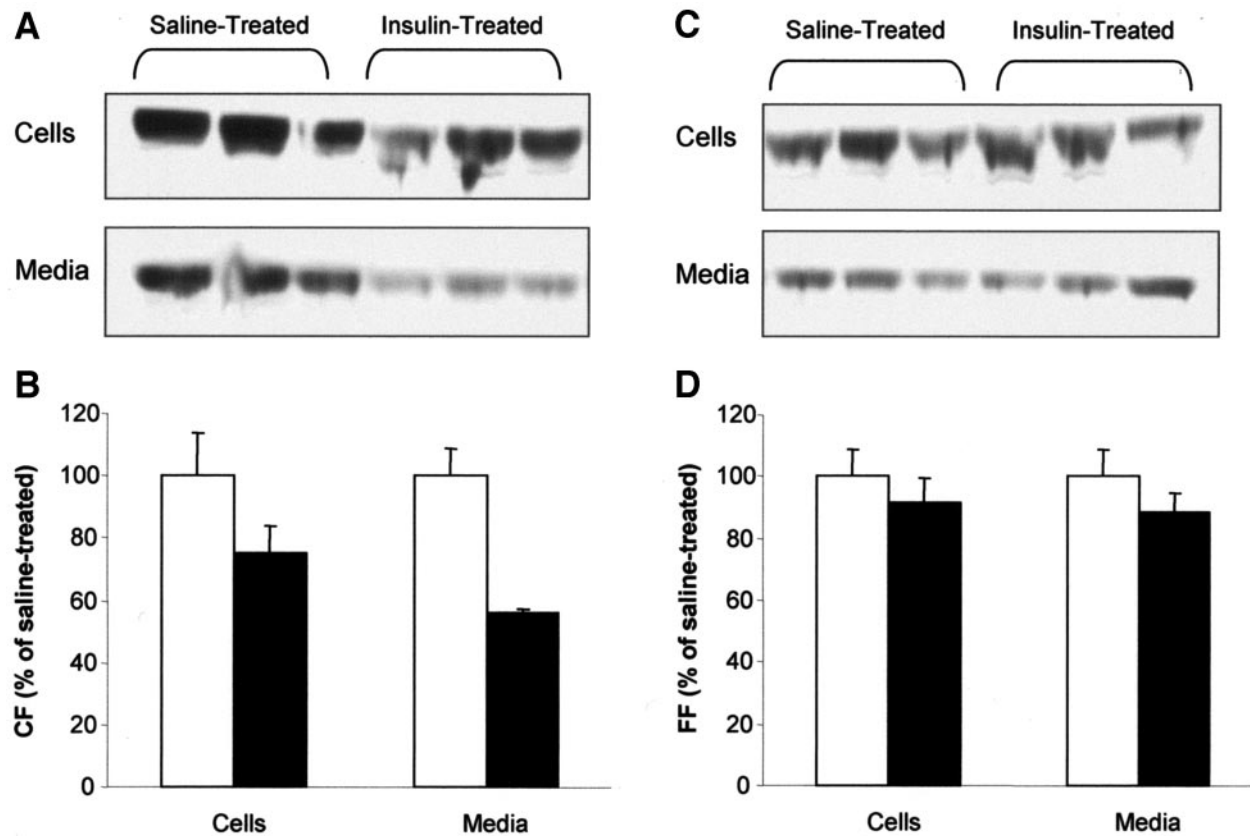


FIG. 2. Insulin treatment in the chow-fed (CF) hamster can decrease intestinal apoB48 secretion but not synthesis. Enterocytes were isolated from saline-treated and insulin-treated chow-fed (A and B) and fructose-fed (FF) (B and C) hamsters. Cells were radiolabeled with [³⁵S]methionine for 60 min, and apoB48 was immunoprecipitated and subjected to SDS-PAGE. ApoB48 was visualized by autoradiography (A and C) and quantified by liquid scintillation counting. Data (means \pm SE) is expressed relative to saline-treated hamster apoB48 synthesis and secretion (B). ■, insulin-treated; □, saline-treated.

able to detect insulin receptor activation through increased tyrosine phosphorylation in both chow-fed and fructose-fed hamster enterocytes. The level of phosphorylated tyrosine was normalized according to the amount of immunoprecipitated insulin receptor. There appeared to be no difference in insulin receptor phosphorylation between enterocytes isolated from chow-fed and fructose-fed hamsters. There also appeared to be no difference between insulin receptor mass in enterocytes from chow-fed and fructose-fed hamsters (Fig. 3A).

Protein expression of IRS-1, p110 subunit of phosphatidylinositol 3-kinase and PTP-1B in enterocytes from chow-fed and fructose-fed hamsters. The protein levels of IRS-1, p110 subunit of phosphatidylinositol (PI) 3-kinase, and PTP-1B were quantified, using immunoblotting. A significant decrease in the expression of IRS-1 was evident in the fructose-fed hamster enterocytes (19%, $P < 0.05$) (Fig. 4A). IRS-1 phosphorylation was also considerably reduced in the fructose-fed hamster enterocytes, resulting in a lower IRS-1p-to-IRS-1 protein mass ratio. There was also a significant increase of 58% in protein expression of the p110 subunit of PI 3-kinase in the fructose-fed hamster intestine ($P < 0.05$) (Fig. 4B). Likewise, there was a significant increase of 36% in PTP-1B expression in the fructose-fed hamster enterocytes ($P < 0.05$) (Fig. 4C). However, only a slight nonsignificant increase (10–15%) in PTP-1B activity was observed (Fig. 4D).

Phosphorylated serine⁴⁷³ Akt and Akt protein expression in chow-fed and fructose-fed hamster en-

terocytes. Using immunoblotting analysis, basal and insulin-stimulated Akt activities were compared in enterocytes from chow-fed and fructose-fed hamsters. Insulin was able to significantly phosphorylate serine⁴⁷³ in both chow-fed and fructose-fed hamster enterocytes. In chow-fed hamster enterocytes, Akt phosphorylation increased 68% after insulin stimulation, whereas in fructose-fed hamsters, Akt phosphorylation increased by 60%. Comparing the chow-fed and fructose-fed hamster enterocytes, no significant differences were observed in basal levels of phosphorylated Akt when levels were normalized according to Akt protein expression (Fig. 5A). Similarly, no significant differences were observed in 10-min 100 nmol/l insulin-stimulated phosphorylated Akt when levels were normalized according to Akt protein expression (Fig. 5A). When analyzing absolute levels of phosphorylated Akt, in the fructose-fed hamster enterocytes, there was a lower trend in the level of phosphorylated Akt that approached significance ($P = 0.09$) (Fig. 5B). Akt protein expression showed a significant decrease of 28% in the fructose-fed hamster enterocytes (Fig. 5C).

Increased basal levels of phosphorylated ERK in fructose-fed hamster enterocytes. To examine the activity of the mitogenic arm of the insulin signaling cascade, phosphorylation and expression of ERK1/2 were quantified. Examining basal levels of phosphorylated ERK, there appeared to be a significant increase of 24% in basal levels of phosphorylated ERK in the fructose-fed hamster ($P < 0.05$) (Fig. 6). Stimulation of enterocytes from chow-fed and fructose-fed hamsters with 100 nmol/l of insulin for 2

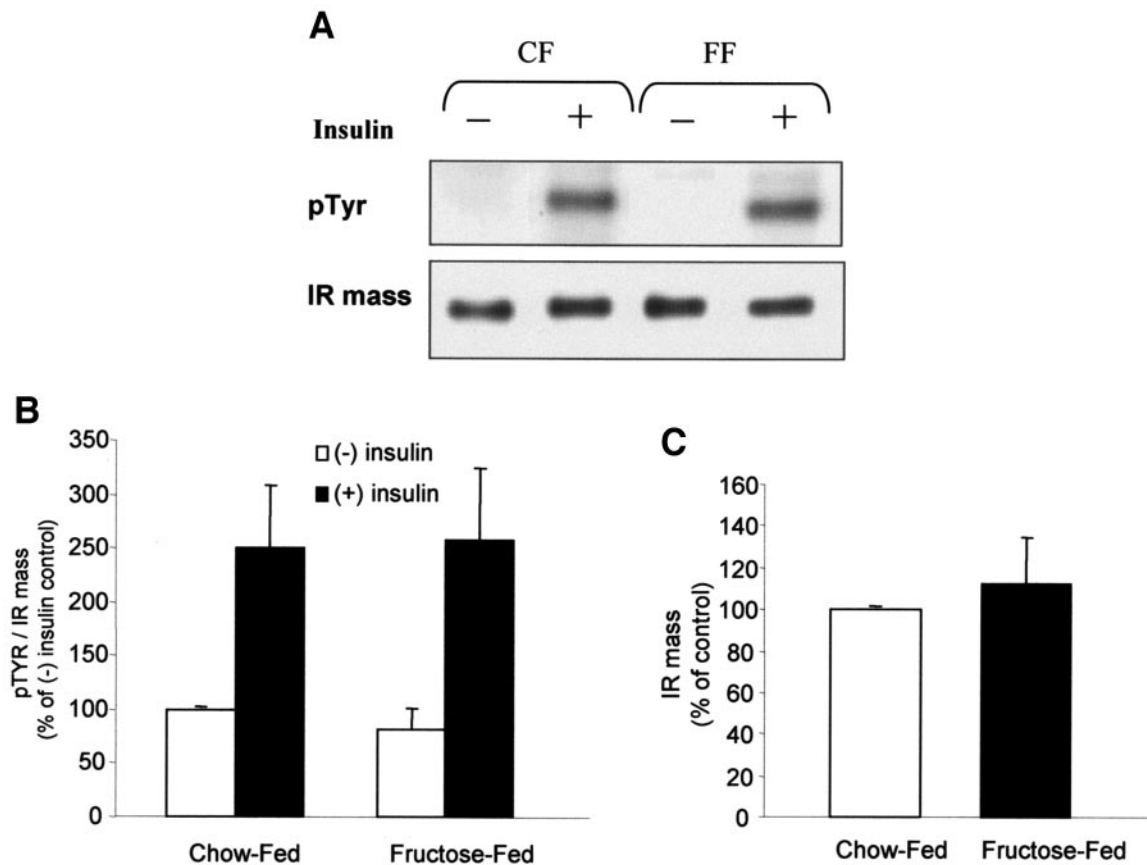


FIG. 3. Tyrosine phosphorylation (pTYR) and protein levels of insulin receptor- β in chow-fed (CF) and fructose-fed (FF) hamster enterocytes. Enterocytes were stimulated with 100 nmol/l insulin for 10 min and then probed for insulin receptor- β phosphorylation and mass. Shown are representative blots (A) as well as graphs of replicate experiments (B and C). Data (means \pm SE, $n = 3$) are expressed relative to control levels. IR, insulin receptor.

min resulted in a significant increase of 78% in phosphorylated levels of ERK in enterocytes from chow-fed hamster enterocytes. This effect was absent in the fructose-fed model, where only a slight increase in phosphorylation resulted in response to insulin stimulation. There was no significant difference in the levels of ERK phosphorylation after 2 min of insulin stimulation in chow-fed and fructose-fed hamster enterocytes (Fig. 6A). There was also no significant difference in ERK protein expression between chow-fed and fructose-fed hamster enterocytes (Fig. 6B). **Mitogen-activated protein/ERK kinase inhibitor PD98059 inhibits phosphorylation of downstream target ERK and intestinal apoB48 production.** To investigate the effects of insulin signaling inhibition on apoB48 production, isolated enterocytes were treated with a highly selective mitogen-activated protein/ERK kinase (MEK) 1/2 inhibitor, PD98059. PD98059 is a useful tool to analyze signal transduction inhibition because it specifically inhibits MEK (26). After a 30-min MEK inhibition in the presence and absence of insulin, cells were pulsed for 2.5 h with [35 S]methionine. MEK inhibition, in the presence or absence of insulin, did not appear to have an effect on cellular levels of apoB48 (Fig. 7A); however, in the presence of insulin, there was a slight but significant decrease (18%, $P = 0.03$) in the secretion of apoB48 into the media (Fig. 7B).

MEK inhibition experiments were also performed in vivo. Hamsters were administered 20 mg/kg PD98059 via intraperitoneal injection. To verify that the intraperitoneal injection of PD98059 reached the target organ and suc-

cessfully inhibited MEK action, the levels of phosphorylation of the downstream target, ERK, were assessed by immunoblotting. Enterocytes were isolated from control and inhibitor-treated hamsters and stimulated with 100 nmol/l insulin for 2 min. Insulin-stimulated, PD98059-treated hamster enterocytes showed a significant inhibition of ERK phosphorylation (Fig. 7C) compared with the control.

Hamsters treated in vivo with PD98059 were used to investigate the effects of insulin signaling inhibition on apoB48 metabolism. Enterocytes were freshly isolated from hamsters treated with DMSO or PD98059 and metabolically labeled. ApoB48 was immunoprecipitated from both cells and media. In PD98059-treated hamsters, a significant decrease of 33% was evident in the cellular levels of apoB48. Similarly, there was a significant decrease of 34% in secreted apoB48 in the PD98059-treated hamster enterocytes compared with enterocytes from DMSO-treated hamsters (Fig. 7D). No difference was observed in total cellular protein synthesis between enterocytes isolated from DMSO-treated and PD98059-treated hamsters (Fig. 7E), suggesting that in vivo treatment with PD98059 at the concentration used did not have a global effect on enterocyte cell viability or protein synthesis activity.

Increased mature form of SREBP-1c in fructose-fed hamster intestine. Evidence from previous studies indicates that fructose-fed hamsters develop increased intestinal fatty acid synthesis (19). There is also evidence suggesting that ERK activation can lead to enhanced

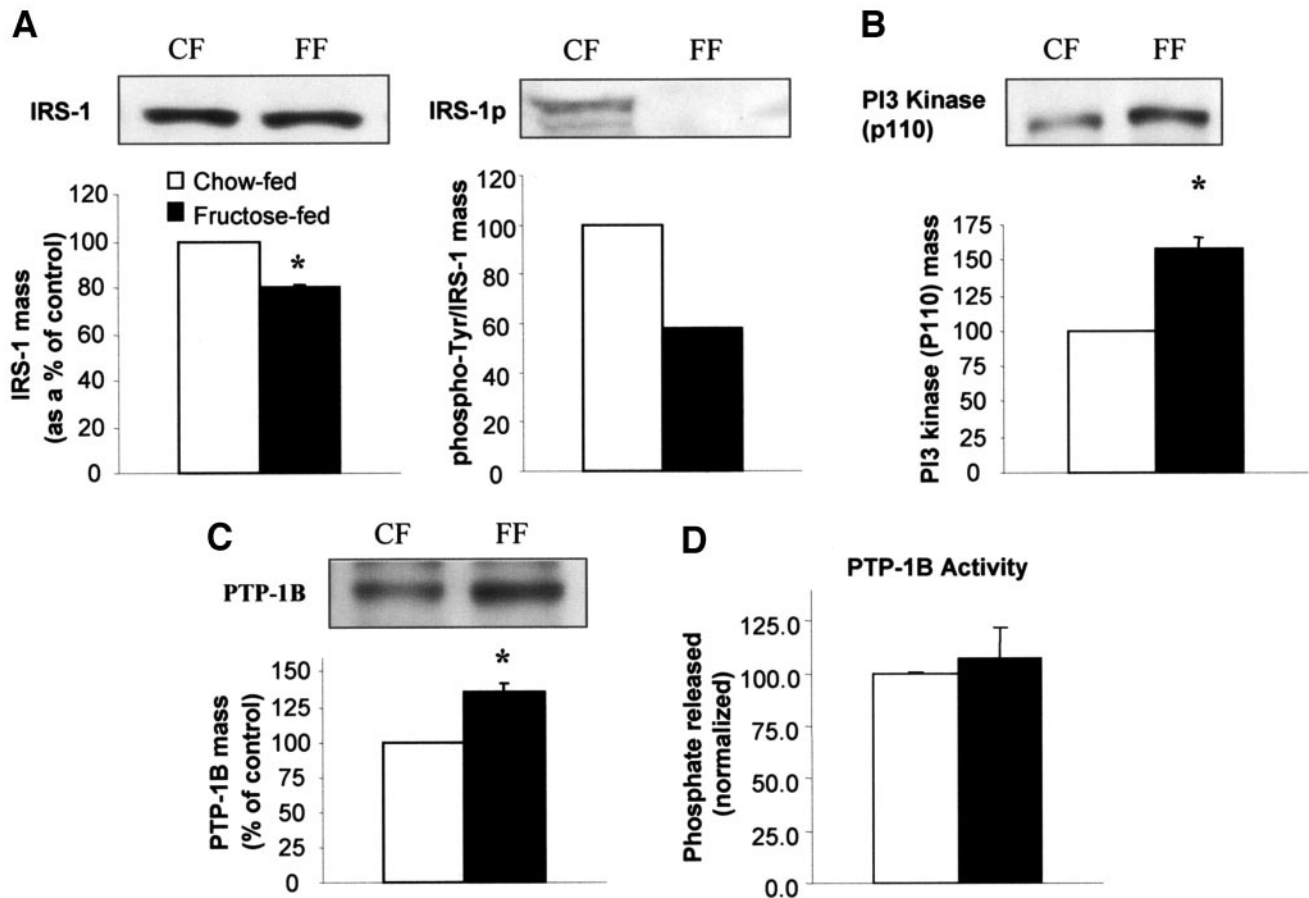


FIG. 4. Tyrosine phosphorylation and protein mass of IRS-1, p110 subunit of PI 3-kinase, and PTP-1B in the chow-fed (CF) and fructose-fed (FF) hamster enterocytes. IRS-1 phosphorylation was assessed by immunoprecipitation of IRS-1 protein followed by immunoblotting with an anti-phosphotyrosine antibody. **A:** Phosphorylated IRS-1 (IRS-1p) and IRS-1 protein mass ($n = 3$). **B:** p110 subunit of PI 3-kinase ($n = 3$). **C:** PTP-1B ($n = 3$). **D:** PTP-1B activity. Data (means \pm SE) are expressed as a percentage of control. Phospho-TYR, phosphorylated tyrosine.

cellular levels of SREBP-1c, an important regulator of lipogenesis. To examine whether the increased rate of fatty acid synthesis that occurs in the fructose-fed hamster intestine is associated with the upregulated transcription factor SREBP-1c, both immature and mature forms of the transcription factor were quantified, using immunoblotting. No difference was observed between the protein mass of the immature SREBP-1c in the enterocytes of chow-fed and fructose-fed hamsters. However, enterocytes isolated from the fructose-fed hamster had a significantly increased level (by 40%, $P = 0.02$) of mature SREBP-1c (Fig. 8).

DISCUSSION

The molecular mechanisms mediating the insulin effect on intestinal lipoprotein metabolism are largely unknown. Indeed, there is almost no information available in the literature on the state of insulin signaling in the intestine during fed and fasting states. Numerous studies have examined the ability of insulin to inhibit hepatocyte-derived apoB100; however, very few studies have investigated the effect of insulin on intestinal apoB48 production. It has been reported by Levy et al. (27) that insulin treatment of cultured jejunal explants from human fetuses causes a reduction in chylomicron production and apoB48 secretion without changes in apoB48 mRNA. It was suggested that the insulin effect was exerted co- or posttranslationally. Insulin did not alter lipid synthesis but reduced

chylomicron production by 29% (28). Tomkin and colleagues (29) have also found that microsomal triglyceride transfer protein mRNA is elevated in insulin-deficient diabetes by threefold resulting in higher lymph chylomicron triglyceride but no change in apoB48 secretion. Our results indicate that insulin can inhibit circulating levels of apoB-containing lipoproteins in the chow-fed hamster and are in agreement with Harbis et al. (30), who reported that postprandial hyperinsulinemia delayed postprandial accumulation of intestinally derived chylomicrons in plasma.

In the current study, the insulin-stimulated inhibition of intestinal apoB48 was also examined in an insulin-resistant animal model, the fructose-fed hamster. Although our laboratory has reported intestinal apoB48 lipoprotein overproduction in the insulin-resistant hamster (9), it was unknown whether this lipoprotein abnormality arises from insensitivity of the intestinal enterocytes to the inhibitory effects of insulin. In vivo and ex vivo studies reported here suggest that, unlike their chow-fed littermates, the fructose-fed hamsters are unresponsive to the inhibitory effects of insulin on apoB48-containing lipoproteins. Ex vivo examination of apoB48 secretion from insulin-treated fructose-fed hamster enterocytes indicated that insulin was unable to inhibit the secretion of apoB48 as in the chow-fed model. Although the insensitivity of hepatic VLDL secretion to the inhibitory effect of insulin has been demonstrated in a number of insulin-resistant animal models (31), this is the first report showing evidence of

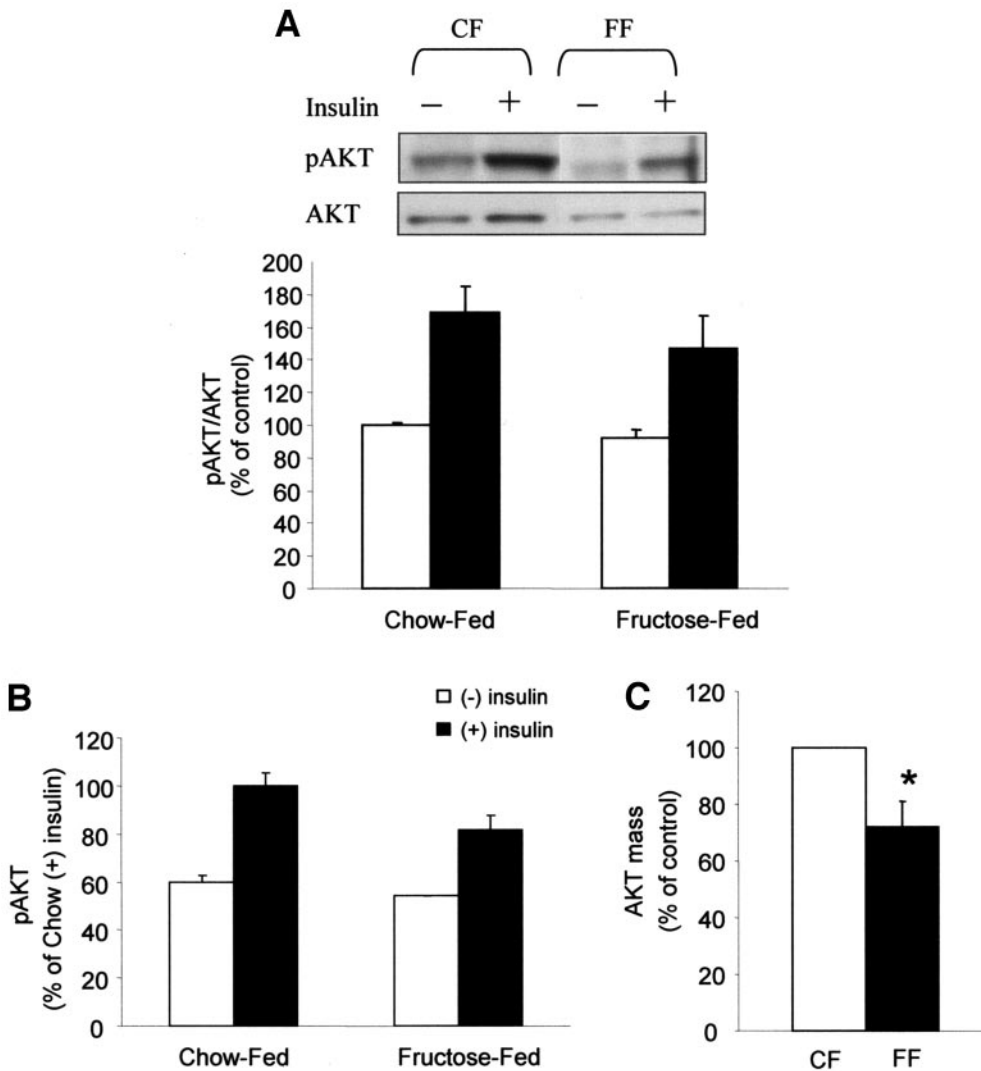


FIG. 5. Serine phosphorylation and protein expression of Akt in chow-fed (CF) and fructose-fed (FF) hamster enterocytes. Enterocytes were stimulated with 100 nmol/l insulin for 10 min and assessed for Akt (serine⁴⁷³) phosphorylation and mass. **A:** Results of phosphorylated Akt (pAKT) normalized to Akt mass (*n* = 3). Data (means ± SE) is expressed as a percentage of non-insulin-stimulated levels of phosphorylation in chow-fed hamster enterocytes. **B:** Levels of phosphorylated Akt. Data (means ± SD) is expressed relative to insulin-stimulated pAkt in chow-fed enterocytes. **C:** Levels of Akt protein mass in chow-fed and fructose-fed enterocytes (*n* = 3). Data (means ± SE) are expressed relative to control levels of Akt mass.

intestinal insulin insensitivity in an animal model of insulin resistance and metabolic dyslipidemia, the fructose-fed hamster.

It should be noted that there were some differences in the insulin sensitivity of enterocytes in *in vivo* versus *ex vivo* experiments. ApoB48 production was clearly sensitive to insulin-mediated inhibition *in vivo*, but there was no insulin effect observed in *ex vivo* studies of isolated enterocytes. These observations may arise from variations in insulin sensitivity of enterocytes *in vivo* versus *ex vivo*. Isolated enterocytes *ex vivo* are less viable and more likely to exhibit aberrant cell signaling responses compared with intact intestinal enterocytes *in vivo* that have maintained their natural anatomy within the intestinal organ. Important factors mediating the insulin effect may also be absent in cultured isolated enterocytes. On the other hand, it is also possible that insulin may indirectly modulate apoB48 production *in vivo*.

Insulin signaling perturbations in insulin-responsive organs such as liver, muscle, and adipose tissues have been well documented in insulin-resistant states (20–24,32). However, this is the first documented study of intestinal insulin signaling during the insulin-resistant state. This study examined the expression and activity of insulin signaling molecules in enterocytes in the fructose-fed hamster model. Our results indicate that the fructose-fed

hamster model had equivalent insulin receptor activity compared with its chow-fed control, indicated by equal tyrosine phosphorylation of insulin receptor-β. There were also no significant differences in insulin receptor-β protein levels. Although many models of insulin resistance show evidence of aberrant insulin signaling at the level of the receptor, some studies have reported normal insulin receptor activity in fructose-fed models. Hyakukoku et al. (33) reported normal insulin receptor-β tyrosine phosphorylation and protein expression in the vasculature and soleus muscle of fructose-fed rats. Bezerra et al. (34) also investigated the insulin signaling pathway in the liver and skeletal muscle and found that stimulation with insulin did not alter the extent of phosphorylation of the insulin receptor in the skeletal muscle of fructose-fed rats compared with control rats.

The activity and expression of downstream signaling molecules were also assessed. It appeared that IRS-1 protein mass and activity were decreased in the fructose-fed hamster model, suggesting that a reduced level of IRs was available for cascading the insulin signal in the fructose-fed hamster. We previously reported decreased IRS-1 protein level in the liver of fructose-fed hamsters (19). Similarly, Desrois et al. (35) have also shown decreased IRS-1 expression in the Goto-Kakizaki rat heart, a strain of glucose-intolerant rat that develops diabetes in

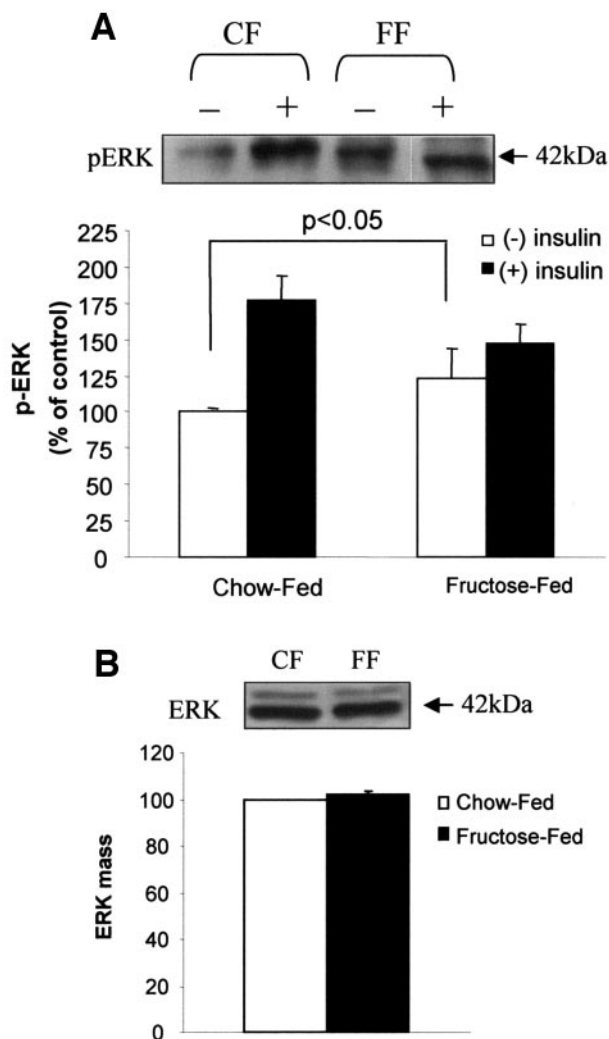


FIG. 6. Tyrosine phosphorylation and protein expression of ERK in chow-fed (CF) and fructose-fed (FF) hamster enterocytes. Enterocytes were stimulated with 100 nmol/l insulin for 2 min, and cell lysates were probed for ERK mass and phosphorylation. **A:** Levels of phosphorylated ERK (p-ERK) in chow-fed and fructose-fed hamster enterocytes ($n = 3$). Data (means \pm SE) is expressed as a percentage of non-insulin-stimulated levels of phosphorylation in chow-fed hamster enterocytes. **B:** Levels of ERK expression in chow-fed and fructose-fed hamster enterocytes ($n = 3$). Data (means \pm SE) are expressed as a percentage of ERK levels in chow-fed hamster enterocytes.

the first few weeks after birth. The mechanism underlying the decreased IRS-1 is unknown but could be caused by increased serine phosphorylation of IRS-1, which has been reported in other animal models of insulin resistance (36,37). Consequently, increased serine phosphorylation of IRS-1 disrupts intracellular distribution of the protein targeting IRS-1 for degradation (38,39).

In the fructose-fed hamster, unexpectedly, there was increased expression of the p110 subunit of PI 3-kinase. The significance of this increased p110 protein mass is unknown, but it may be a compensatory response to downregulated insulin signaling cascade in this model. Further downstream the PI 3-kinase pathway, insulin was able to significantly increase phosphorylated Akt in both chow-fed and fructose-fed hamster enterocytes. However, basal levels and insulin-stimulated serine phosphorylation of Akt, normalized against Akt protein mass, were not significantly different between chow-fed and fructose-fed hamster enterocytes. Yet, protein expression of Akt was

significantly decreased in the fructose-fed hamster enterocytes. We have previously reported that hepatocytes from fructose-fed hamsters dramatically reduced Akt serine phosphorylation (19). These results were in agreement with findings from Krook et al. (40) and Rondinone et al. (41), who also reported impaired Akt phosphorylation in muscle and adipose tissue of insulin-resistant diabetic subjects. Interestingly, increased expression of PTP-1B, a negative regulator of the insulin signaling pathway, was observed in the fructose-fed hamster model, similar to our recent observations in fructose-fed hamster hepatocytes (41). The increased PTP-1B protein mass was not accompanied by a significant increase in PTP-1B activity (only a nonsignificant trend toward increased activity was observed). The data appears to suggest that fructose feeding does induce increases in protein mass of PTP-1B with only minimal effects on the activity, which may potentially explain the presence of normal activity of the insulin receptor in the face of increased PTP-1B protein mass.

We also assessed the activity and protein mass of ERK1/2 in the intestine of chow-fed and fructose-fed hamsters. First, the mitogen-activated protein (MAP) kinase pathway in intestinal enterocytes appeared to be responsive to insulin stimulation because insulin was able to significantly stimulate phosphorylation of ERK1/2 in the normal, chow-fed hamster. However, in the fructose-fed hamster model, intestinal ERK1/2 was not as responsive to insulin because only a slight and insignificant increase in phosphorylation was observed compared with basal levels. These results indicate that the insulin-resistant fructose-fed hamster has aberrant intestinal insulin signaling on the mitogenic arm of the signaling cascade. Interestingly, however, in the fructose-fed hamster, there was a significant increase in basal levels of ERK1/2 phosphorylation. Increased basal levels of phosphorylated ERK1/2 have also been seen in the microvessels of epididymal fat in obese Zucker rats (42), in hepatocytes of *ob/ob* mice relative to lean *ob/+* littermates (43), and in adipocytes of type 2 diabetic patients (44). The increase in basal levels of phosphorylated ERK1/2 could be attributed to increased activity of inflammatory pathways that are believed to interfere with insulin signaling (45). Recent evidence suggests that insulin resistance is strongly associated with an inflammatory response, particularly, an increase in the cytokine tumor necrosis factor (TNF)- α . TNF- α is an important modulator of energy metabolism, and increased levels of TNF- α have been shown in obesity and non-insulin-dependent diabetes (46). TNF- α plays a role in kinase signaling by activating p42/44 ERK (47). Although proinflammatory cytokines have not yet been investigated in the fructose-fed model (because of lack of a specific hamster TNF- α assay), increased levels of TNF- α could be responsible for increased basal levels of ERK1/2 phosphorylation.

We also examined the potential role of the MAP kinase pathway in the regulation of apoB48 using an *in vivo* model of MEK inhibition. MEK1/2 inhibition in the hamster resulted in decreased intestinal production of apoB48 in hamster enterocytes, suggesting a link between insulin signaling and lipoprotein production at the level of the intestine. The mechanisms linking ERK activity and intestinal lipoprotein secretion are currently known. It has been demonstrated that the MAP kinase cascade is linked to SREBPs (48,49). ERK1/2 has been shown to activate SREBP-1a by phosphorylating serine¹¹⁷ (50). SREBPs bind to sterol responsive elements found on multiple genes, and thus they can activate a cascade of enzymes in-

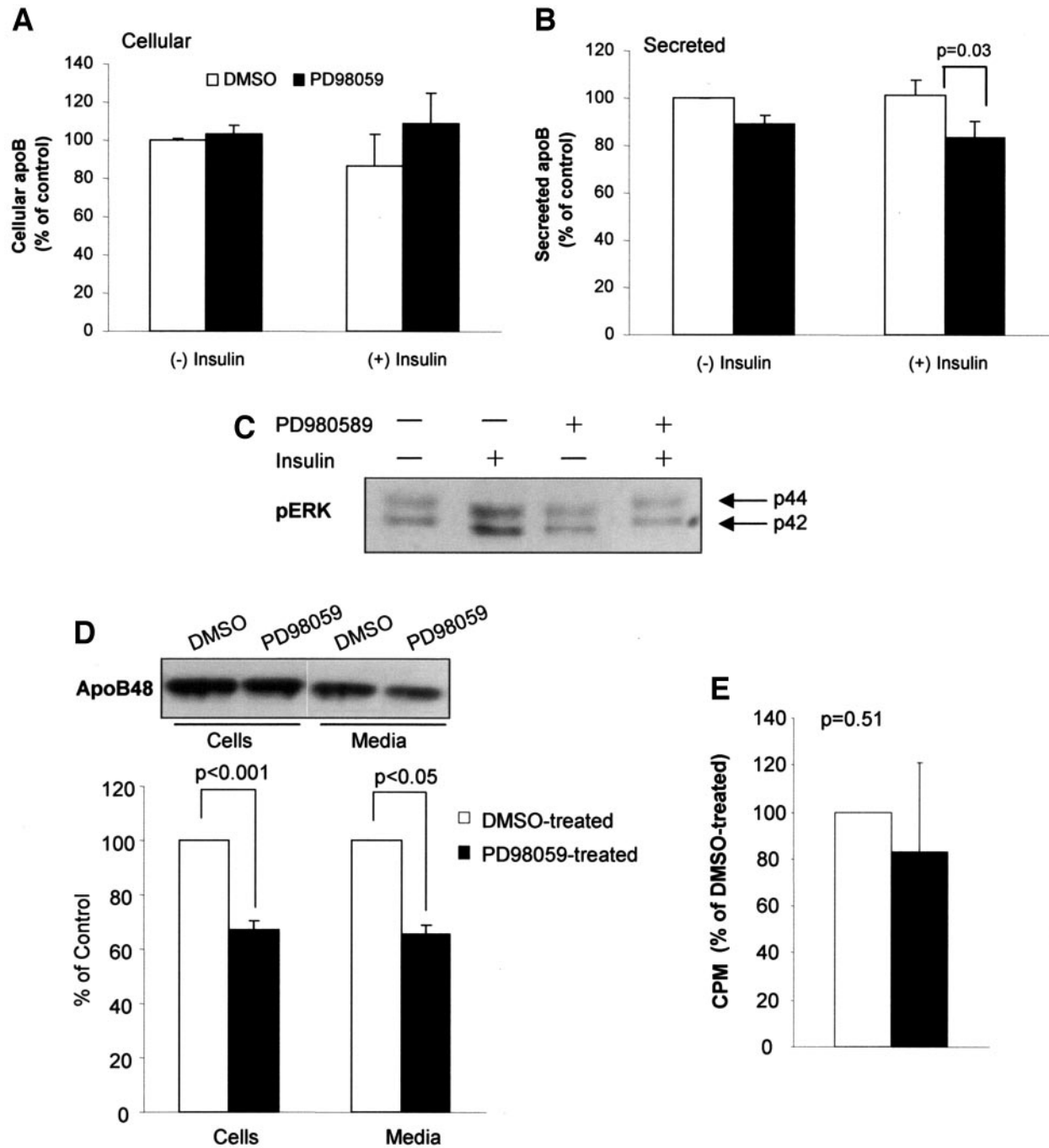


FIG. 7. MEK1/2 inhibitor PD98059 inhibits ERK phosphorylation and apoB48 production. In ex vivo experiments, isolated enterocytes were treated with MEK1/2 inhibitor, PD98059, in the presence and absence of insulin followed by assessment of apoB48 synthesis and secretion (A and B). In in vivo experiments, hamsters were injected with MEK1/2 inhibitor PD98059 (20 mg/kg i.p.) or the vehicle DMSO. C: Isolated enterocytes were stimulated with 100 nmol/l insulin and probed for phosphorylated ERK (pERK; Tyr204). D: Enterocytes were radiolabeled with [³⁵S]methionine, and apoB48 was immunoprecipitated and subjected to SDS-PAGE and autoradiography. ApoB counts were normalized to total radiolabeled protein count (n = 3). E: Total radiolabeled protein levels in enterocytes from DMSO-treated and PD98059-treated hamsters.

involved in cholesterol and lipid biosynthetic pathways, such as hydroxymethylglutaryl-CoA reductase and fatty acid synthase, respectively. Insulin has been shown to activate SREBPs through the MAP kinase pathway (51). ERK-mediated upregulation of SREBP may explain the stimulated lipoprotein production in the fructose-fed model because SREBP activation has been shown to increase apoB secretion (52,53). We also observed a significant increase in the mature form of SREBP-1c in intestinal enterocytes from the fructose-fed hamsters, sug-

gesting activation of the SREBP-1c pathway in this model. Concomitant increases in basal activities of both ERK and SREBP-1c suggest a potential causative link between these two processes, which together may be responsible for the previously reported enhanced rate of de novo lipogenesis in the intestine of the fructose-fed hamster model. Interestingly, a link has also been demonstrated between PTP-1B and SREBP regulation. In insulin-resistant fructose-fed rats, Nagai et al. (54) identified a strong correlation between increased PTP-1B and SREBP-1 mRNA in the

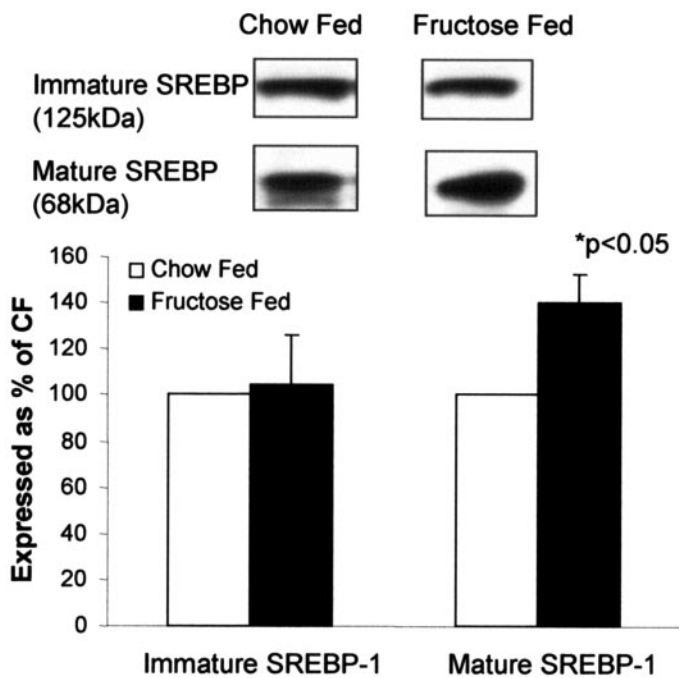


FIG. 8. Fructose feeding induces SREBP-1 activation in fructose-fed hamster intestine. Microsomes were prepared from freshly isolated enterocytes and solubilized in cell-solubilizing buffer, and then 50 μ g of cell lysate was subjected to SDS-PAGE, transferred to polyvinylidene difluoride membrane, and immunoblotted with an anti-hamster SREBP-1 antibody (1:1,000-fold dilution). Data are means \pm SD and are presented as a percentage of chow-fed SREBP-1 ($n = 3$).

liver. When PTP-1B was overexpressed in rat hepatocytes, it led to increased mRNA content and promoter activity of SREBP-1a and -1c. The authors suggested a role for PTP-1B in enhancing SREBP-1 gene expression through upregulating Sp1 transcriptional activity via an increase in protein phosphatase 2A activity (55).

In conclusion, the unresponsiveness of intestinal lipoprotein production to the inhibitory effects of insulin and the aberrant insulin signaling in the fructose-fed hamster model suggest the development of insulin resistance at the level of the intestine with high fructose feeding. Upregulation of the ERK pathway in response to inflammatory factors such as TNF- α may lead to SREBP-1c activation in intestinal enterocytes and may induce intestinal lipoprotein production and postprandial dyslipidemia in the fructose-fed model. Further investigation is underway to examine the molecular basis linking ERK activation, SREBP function, de novo lipogenesis, and the assembly and secretion of apoB48-lipoprotein particles in intestinal enterocytes.

ACKNOWLEDGMENTS

This work was supported by an operating grant from the Canadian Institutes of Health Research (to K.A.).

REFERENCES

- Grundy SM, Brewer HB Jr, Cleeman JI, Smith SC Jr, Lenfant C: Definition of metabolic syndrome: report of the National Heart, Lung, and Blood Institute/American Heart Association conference on scientific issues related to definition. *Arterioscler Thromb Vas Biol* 24:e13–e18, 2004
- Beckman JA, Creager MA, Libby P: Diabetes and atherosclerosis: epidemiology, pathophysiology, and management. *JAMA* 287:2570–2581, 2002
- Moller DE, Flier JS: Insulin resistance: mechanisms, syndromes, and implications. *N Engl J Med* 325:938–948, 1991
- Eschwege E, Richard JL, Thibault N, Ducimetiere P, Warnet JM, Claude JR, Rosselin GE: Coronary heart disease mortality in relation with diabetes, blood glucose and plasma insulin levels: the Paris Prospective Study, ten years later. *Horm Metab Res Suppl* 15:41–46, 1985
- Gu K, Cowie CC, Harris MI: Diabetes and decline in heart disease mortality in US adults. *JAMA* 281:1291–1297, 1999
- Mero N, Syvanne M, Taskinen MR: Postprandial lipid metabolism in diabetes. *Atherosclerosis* 141 (Suppl. 1):S53–S55, 1998
- Curtin A, Deegan P, Owens D, Collins P, Johnson A, Tomkin GH: Elevated triglyceride-rich lipoproteins in diabetes: a study of apolipoprotein B-48. *Acta Diabetol* 33:205–210, 1996
- Taskinen MR: Diabetic dyslipidaemia: from basic research to clinical practice. *Diabetologia* 46:733–749, 2003
- Haidari M, Leung N, Mahbub F, Uffelman KD, Kohen-Avramoglu R, Lewis GF, Adeli K: Fasting and postprandial overproduction of intestinally derived lipoproteins in an animal model of insulin resistance: evidence that chronic fructose feeding in the hamster is accompanied by enhanced intestinal de novo lipogenesis and ApoB48-containing lipoprotein overproduction. *J Biol Chem* 277:31646–31655, 2002
- Phillips C, Madigan C, Owens D, Collins P, Tomkin GH: Defective chylomicron synthesis as a cause of delayed particle clearance in diabetes? *Int J Exp Diabetes Res* 3:171–178, 2002
- Phillips C, Bennett A, Anderton K, Owens D, Collins P, White D, Tomkin GH: Intestinal rather than hepatic microsomal triglyceride transfer protein as a cause of postprandial dyslipidemia in diabetes. *Metabolism* 51:847–852, 2002
- Zilverman DB: Atherogenesis: a postprandial phenomenon. *Circulation* 60:473–485, 1979
- Kane JP: Apolipoprotein B: structural and metabolic heterogeneity. *Annu Rev Physiol* 45:637–650, 1983
- Sparks JD, Sparks CE: Insulin modulation of hepatic synthesis and secretion of apolipoprotein B by rat hepatocytes. *J Biol Chem* 265:8854–8862, 1990
- Zoltowska M, Ziv E, Delvin E, Sinnott D, Kalman R, Garofalo C, Seidman E, Levy E: Cellular aspects of intestinal lipoprotein assembly in *Psammomys obesus*: a model of insulin resistance and type 2 diabetes. *Diabetes* 52:2539–2545, 2003
- Curtin A, Deegan P, Owens D, Collins P, Johnson A, Tomkin GH: Alterations in apolipoprotein B-48 in the postprandial state in NIDDM. *Diabetologia* 37:1259–1264, 1994
- Kohen-Avramoglu R, Theriault A, Adeli K: Emergence of the metabolic syndrome in childhood: an epidemiological overview and mechanistic link to dyslipidemia. *Clin Biochem* 36:413–420, 2003
- Taghibiglou C, Carpentier A, Van Iderstine SC, Chen B, Rudy D, Aiton A, Lewis GF, Adeli K: Mechanisms of hepatic very low density lipoprotein overproduction in insulin resistance: evidence for enhanced lipoprotein assembly, reduced intracellular ApoB degradation, and increased microsomal triglyceride transfer protein in a fructose-fed hamster model. *J Biol Chem* 275:8416–8425, 2000
- Taghibiglou C, Rashid-Kolvear F, Van Iderstine SC, Le Tien H, Fantus IG, Lewis GF, Adeli K: Hepatic very low density lipoprotein-ApoB overproduction is associated with attenuated hepatic insulin signaling and overexpression of protein-tyrosine phosphatase 1B in a fructose-fed hamster model of insulin resistance. *J Biol Chem* 277:793–803, 2002
- Bjornholm M, Kawano Y, Lehtihet M, Zierath JR: Insulin receptor substrate-1 phosphorylation and phosphatidylinositol 3-kinase activity in skeletal muscle from NIDDM subjects after in vivo insulin stimulation. *Diabetes* 46:524–527, 1997
- Goodyear LJ, Giorgino F, Sherman LA, Carey J, Smith RJ, Dohm GL: Insulin receptor phosphorylation, insulin receptor substrate-1 phosphorylation, and phosphatidylinositol 3-kinase activity are decreased in intact skeletal muscle strips from obese subjects. *J Clin Invest* 95:2195–2204, 1995
- Rondinone CM, Wang LM, Lonroth P, Wesslau C, Pierce JH, Smith U: Insulin receptor substrate (IRS) 1 is reduced and IRS-2 is the main docking protein for phosphatidylinositol 3-kinase in adipocytes from subjects with non-insulin-dependent diabetes mellitus. *Proc Natl Acad Sci U S A* 94:4171–4175, 1997
- Zierath JR, Krook A, Wallberg-Henriksson H: Insulin action in skeletal muscle from patients with NIDDM. *Mol Cell Biochem* 182:153–160, 1998
- Caro JF, Ittoop O, Pories WJ, Meelheim D, Flickinger EG, Thomas F, Jenquin M, Silverman JF, Khazanie PG, Sinha MK: Studies on the mechanism of insulin resistance in the liver from humans with noninsulin-dependent diabetes: insulin action and binding in isolated hepatocytes, insulin receptor structure, and kinase activity. *J Clin Invest* 78:249–258, 1986
- Taggart C, Gibney J, Owens D, Collins P, Johnson A, Tomkin GH: The role

- of dietary cholesterol in the regulation of postprandial apolipoprotein B48 levels in diabetes. *Diabet Med* 14:1051-1058, 1997
26. Alessi DR, Cuenda A, Cohen P, Dudley DT, Saltiel AR: PD 098059 is a specific inhibitor of the activation of mitogen-activated protein kinase in vitro and in vivo. *J Biol Chem*. 270:27489-27494, 1995
 27. Levy E, Sinnott D, Thibault L, Nguyen TD, Delvin E, Menard D: Insulin modulation of newly synthesized apolipoproteins B-100 and B-48 in human fetal intestine: gene expression and mRNA editing are not involved. *FEBS Lett* 393:253-258, 1996
 28. Loirdighi N, Menard D, Levy E: Insulin decreases chylomicron production in human fetal small intestine. *Biochim Biophys Acta* 1175:100-106, 1992
 29. Gleeson A, Anderton K, Owens D, Bennett A, Collins P, Johnson A, White D, Tomkin GH: The role of microsomal triglyceride transfer protein and dietary cholesterol in chylomicron production in diabetes. *Diabetologia* 42:944-948, 1999
 30. Harbis A, Defoort C, Narbonne H, Juhel C, Senft M, Latge C, Delenne B, Portugal H, Atlan-Gepner C, Vialettes B, Lairon D: Acute hyperinsulinism modulates plasma apolipoprotein B-48 triglyceride-rich lipoproteins in healthy subjects during the postprandial period. *Diabetes* 50:462-469, 2001
 31. Sparks JD, Sparks CE: Obese Zucker (fa/fa) rats are resistant to insulin's inhibitory effect on hepatic apo B secretion. *Biochem Biophys Res Commun* 205:417-422, 1994
 32. Michael MD, Kulkarni RN, Postic C, Previs SF, Shulman GI, Magnuson MA, Kahn CR: Loss of insulin signaling in hepatocytes leads to severe insulin resistance and progressive hepatic dysfunction. *Mol Cell* 6:87-97, 2000
 33. Hyakukoku M, Higashiura K, Ura N, Murakami H, Yamaguchi K, Wang L, Furuhashi M, Togashi N, Shimamoto K: Tissue-specific impairment of insulin signaling in vasculature and skeletal muscle of fructose-fed rats. *Hypertens Res* 26:169-176, 2003
 34. Bezerra RM, Ueno M, Silva MS, Tavares DQ, Carvalho CR, Saad MJ: A high fructose diet affects the early steps of insulin action in muscle and liver of rats. *J Nutr* 130:1531-1535, 2000
 35. Desrois M, Sidell RJ, Gauguier D, King LM, Radda GK, Clarke K: Initial steps of insulin signaling and glucose transport are defective in the type 2 diabetic rat heart. *Cardiovasc Res* 61:288-296, 2004
 36. Qiao LY, Goldberg JL, Russell JC, Sun XJ: Identification of enhanced serine kinase activity in insulin resistance. *J Biol Chem* 274:10625-10632, 1999
 37. Werner ED, Lee J, Hansen L, Yuan M, Shoelson SE: Insulin resistance due to phosphorylation of IRS-1 at serine 302. *J Biol Chem* 279:35298-35305, 2004
 38. Clark SF, Molero JC, James DE: Release of insulin receptor substrate proteins from an intracellular complex coincides with the development of insulin resistance. *J Biol Chem* 275:3819-3826, 2000
 39. Sun XJ, Goldberg JL, Qiao LY, Mitchell JJ: Insulin-induced insulin receptor substrate-1 degradation is mediated by the proteasome degradation pathway. *Diabetes* 48:1359-1364, 1999
 40. Krook A, Roth RA, Jiang XJ, Zierath JR, Wallberg-henriksson H: Insulin-stimulated Akt kinase activity is reduced in skeletal muscle from NIDDM subjects. *Diabetes* 47:1281-1286, 1998
 41. Rondinone CM, Carvalho E, Wesslau C, Smith UP: Impaired glucose transport and protein kinase B activation by insulin, but not okadaic acid, in adipocytes from subjects with type II diabetes mellitus. *Diabetologia* 42:819-825, 1999
 42. Jiang ZY, Lin YW, Clemont A, Feener EP, Hein KD, Igarashi M, Yamauchi T, White MF, King GL: Characterization of selective resistance to insulin signaling in the vasculature of obese Zucker (fa/fa) rats. *J Clin Invest* 104:447-457, 1999
 43. Gum RJ, Gaede LL, Heindel MA, Waring JF, Trevillyan JM, Zinker BA, Stark ME, Wilcox D, Jirousek MR, Rondinone CM, Ulrich RG: Antisense protein tyrosine phosphatase 1B reverses activation of p38 mitogen-activated protein kinase in liver of ob/ob mice. *Mol Endocrinol* 17:1131-1143, 2003
 44. Carlson CJ, Koterski S, Sciotti RJ, Pocard GB, Rondinone CM: Enhanced basal activation of mitogen-activated protein kinases in adipocytes from type 2 diabetes: potential role of p38 in the downregulation of GLUT4 expression. *Diabetes* 52:634-641, 2003
 45. Hotamisligil GS: Inflammatory pathways and insulin action. *Int J Obes Relat Metab Disord* 27 (Suppl. 3):S53-S55, 2003
 46. Hotamisligil GS, Shargill NS, Spiegelman BM: Adipose expression of tumor necrosis factor-alpha: direct role in obesity-linked insulin resistance. *Science* 259:87-91, 1993
 47. Engelman JA, Berg AH, Lewis RY, Lisanti MP, Scherer PE: Tumor necrosis factor alpha-mediated insulin resistance, but not dedifferentiation, is abrogated by MEK1/2 inhibitors in 3T3-L1 adipocytes. *Mol Endocrinol* 14:1557-1569, 2000
 48. Kotzka J, Muller-Wieland D, Roth G, Kremer L, Munck M, Schurmann S, Knebel B, Krone W: Sterol regulatory element binding proteins (SREBP)-1a and SREBP-2 are linked to the MAP-kinase cascade. *J Lipid Res* 41:99-108, 2000
 49. Kotzka J, Muller-Wieland D, Koponen A, Njamen D, Kremer L, Roth G, Munck M, Knebel B, Krone W: ADD1/SREBP-1c mediates insulin-induced gene expression linked to the MAP kinase pathway. *Biochem Biophys Res Commun* 249:375-379, 1998
 50. Roth G, Kotzka J, Kremer L, Lehr S, Lohaus C, Meyer HE, Krone W, Muller-Wieland D: MAP kinases Erk1/2 phosphorylate sterol regulatory element-binding protein (SREBP)-1a at serine 117 in vitro. *J Biol Chem* 275:33302-33307, 2000
 51. Streicher R, Kotzka J, Muller-Wieland D, Siemeister G, Munck M, Avci H, Krone W: SREBP-1 mediates activation of the low density lipoprotein receptor promoter by insulin and insulin-like growth factor-I. *J Biol Chem* 271:7128-7133, 1996
 52. Elam MB, Wilcox HG, Cagen LM, Deng X, Raghov R, Kumar P, Heimberg M, Russell JC: Increased hepatic VLDL secretion, lipogenesis, and SREBP-1 expression in the corpulent JCR:LA-cp rat. *J Lipid Res* 42:2039-2048, 2001
 53. Wang SL, Du EZ, Martin TD, Davis RA: Coordinate regulation of lipogenesis, the assembly and secretion of apolipoprotein B-containing lipoproteins by sterol response element binding protein 1. *J Biol Chem* 272:19351-19358, 1997
 54. Nagai Y, Nishio Y, Nakamura T, Maegawa H, Kikkawa R, Kashiwagi A: Amelioration of high fructose-induced metabolic derangements by activation of PPARalpha. *Am J Physiol Endocrinol Metab* 282:E1180-E1190, 2002
 55. Shimizu S, Ugi S, Maegawa H, Egawa K, Nishio Y, Yoshizaki T, Shi K, Nagai Y, Morino K, Nemoto K, Nakamura T, Bryer-Ash M, Kashiwagi A: Protein-tyrosine phosphatase 1B as new activator for hepatic lipogenesis via sterol regulatory element-binding protein-1 gene expression. *J Biol Chem* 278:43095-43101, 2003